Heliyon 10 (2024) e33755

Contents lists available at ScienceDirect

Heliyon

journal homepage: www.cell.com/heliyon

Research article

Immune suppressive drugs negatively regulate the CD8^{+}T cells function by acetyltransferase p300 induced canonical and non-canonical autophagy

Runfeng Ni [a,b,1], Liwei Fan [a,c,1], Haijin Wang [a,1], Quan Zhang [a], Le Zhang [a,d], Aidi Wang [a,**], Baoshan Liu [a,*]

[a] *Department of Traditional Chinese Medicine, Tianjin Medical University General Hospital, Tianjin, 300052, China*
[b] *Department of Hematology, Shanghai Municipal Hospital of Traditional Chinese Medicine, Shanghai University of Traditional Chinese Medicine, Shanghai, 200071, China*
[c] *Xiasha Street Community Healthcare Center, Hangzhou, 310018, China*
[d] *Department of Dermatology, Air Force Medical Center, PLA, Beijing, 100142, China*

ARTICLE INFO

Keywords:
Canonical/non-canonical autophagy
mTORC1
p300
CD8^{+}T cells
Cyclosporin A
Dioscin
Aplastic anemia

ABSTRACT

Macroautophagy, the mainly regulated form of autophagy, maintains the cellular homeostasis and degrades the transported cargoes. It is initiated by the protein kinase complex regulating by two signals pathway Mammalian target of rapamycin complex 1 (mTORC1)-Adenosine 5' monophosphate activated protein kinase (AMPK)-Unc 51 like kinase 1(ULK1) and ULK1-PI3K-phosphatidylinositol 3-phosphate (PI3P). Currently, autolysosomes are accumulated during the aging process of CD8^{+}T cells in vitro and may participate in inducing death sensitization of senescent cells. The main mechanism of aplastic anemia, a hyperimmune disease, is the T cells subsets imbalance such as CD8^{+}T cells abnormal activation and hyperfunction. Therefore, the role of autophagy in the CD8^{+}T cells and supposed whether some immunosuppress drugs induced the cells autophagic death to treat the hyperimmune diseases were focused. It was decided found that the acetyltransferase p300 obviously increased in the aplastic anemia patients and was related with the severity of disease. Previous studies have reported that canonical autophagy is regulated by the mTORC1-p300 axis. p300 is a critical bridge in the p300-VPS34 axis mediated non-canonical autophagy. There is the deficiency of autophagy and acetylation in the CD8^{+}T cells. The expression of p300 also decreased notably after the immunosuppressive drugs therapy. Our findings provide a framework for understanding how immunosuppressive drugs effect on the AA autophagy deficiency mechanism and proved that immunosuppressive drugs negatively regulated the function of CD8^{+}T cells by p300-mediated canonical autophagy pathway and non-canonical autophagy pathway.

Abbreviations: mTOR, mechanistic target of rapamycin; mTORC1, mammalian target of rapamycin complex 1; EP300/p300, E1A binding protein p300; IST, immunosuppressive therapy; RAPA, rapamycin; TSC, tuberous sclerosis complex 2; AMPK, AMP-activated protein kinase; VPS34, vacuolar protein sorting 34; LC3II, microtubule-associated protein 1 light chain 3II; LC3B, microtubule-associated protein 1 light chain 3β; p62, sequestosome 1; AA, aplastic anemia; Atg, autophagy related gene; GZMS-B, Granzyme B; TNF-α, Tumor Necrosis Factor α; IFN-γ, Interferon-gamma; CD, cluster of differentiation; CsA, Cyclosporin A; DNS, Dioscin; ISC, Immunosuppressive Compound; ELISA, enzyme-linked immunosorbent assay; CCK-8, cell counting kit-8.

* Corresponding author
** Corresponding author
[1] These authors contributed equally to this study.

https://doi.org/10.1016/j.heliyon.2024.e33755
Received 28 January 2024; Received in revised form 25 June 2024; Accepted 26 June 2024
Available online 29 June 2024

1. Introduction

Aplastic Anemia, a bone marrow failure disease, was characterized by peripheral allogeneic cytopenia and hyperproliferative bone marrow. The main mechanism of AA is the abnormal activation and hyperfunction of $CD8^+$T cells. and immunosuppressive therapy (IST), such as the first-line treatment of antihuman thymocyte globulin (ATG) combined with Cyclosporin A (CsA), has achieved good efficacy, which also confirms the close relationship between AA and immunity [1,2]. However, there are many side effects and the recurrence rate of immunosuppressive therapy (IST) and nearly 30 % of patients are tolerant to IST, which seriously threatens the survival rate and quality of life. Therefore, it is urgent to explore new therapeutic strategies and drug target for the pathogenesis of AA.

Autophagy, a cellular state under starvation and stress, has evolved with scientific research from being described initially as a nonselective mechanism for intracellular waste disposal and recycling to being regarded as a highly selective and highly conserved cell survival program in mammals to maintain homeostasis in cells and tissues, which is relevant to the basic survival metabolic processes of cells [3]. Therefore, the optimal use of the role of autophagy in the cell is critical. According to our team previous research, Dioscin (DNS) regulated the autophagy level of the bone marrow cells in AA. In this study, we researched the immune suppressive compound, DNS combined with CsA, to further illustrate the importance of autophagy in the AA immune homeostasis. Abnormal autophagy states have been identified in the mechanism of aplastic anemia, a recent study have shown impaired autophagy of $CD34^+$cells in the bone marrow of AA patients [4], so we speculated whether there is a autophagy deficiency induced abnormally activated $CD8^+$T cells in the pathogenesis of AA?

In our study, we illustrated the macroautophagy in AA. Acetylation was a crucial regulator step in autophagy [5]. Previous studyfound that p300 increased in the $CD8^+$T cells of the severe aplastic anemia immune pathogenesis [6,7]. p300, a direct target of mTORC1, inhibited autophagy to activate mTORC1 by phosphorylating the serine residue at the carboxyl terminus of p300 [8]. Therefore, we first investigated a potential role of immunosuppressive drugs in the mTORC1-p300 pathway mediated canonical autophagy to regulate the mTOR itself activity and its substrate p300 activity to further effect the expression of autophagy-related proteins such as microtubule-associated protein 1 light chain 3 (LC3), autophagy related gene (Atg) and p62 [9]. Our results demonstrated that immunosuppressive compound (ISC) had effect on inhibiting the mTORC1 activity, notably, not only did decrease the activity of p300 but the expression of p300 also decreased after the ISC intervening. We then supposed that whether ISC directly target on the p300 and initiate the non-canonical autophagy by the p300-Vacuolar protein sorting 34(VPS34) pathway. The results showed that ISC inhibited the expression and activity of p300 and its substrate VPS34 deacetylation increased to further induce the non-canonical autophagy. Here, we focused on the role of ISC target on the acetyltransferase p300 mediated upstream and substrate in inducing the canonical autophagy and non-canonical autophagy. Finally, we investigated the immunosuppressive drugs played a critical role in the $CD8^+$T cells autophagy initiation to treat the AA hyperimmune function. It was demonstrated that ISC induced CD8+T cells autophagy, our results showed that CD25, CD44, CD69 and TCR cell surface molecular were decreased, inflammatory cytokines showed downregulation and it was consistent with the previous studies that interleukins and Toll-like receptors (TLRs) play a vital role in the immune system molecules and cells and were found critical in the prognosis of AA [10,11]. In short, ISC induced the canonical and non-canonical autophagy of $CD8^+$T to inhibit it activity and function for treating AA.

2. Materials and methods

2.1. Animal model

To establish aplastic anemia mice model, Balb/C male mice were chosen as recipient mouse and DBA/2 male mice were chosen as donor mouse. AA model was constructed by a sublethal total body irradiation dose combined with allogeneic lymphocyte infusion. Balb/C mice were randomly separated to two groups, the model group and Ctrl group. Mice in model group were accepted total body irradiation with sublethal dosage 5 Gy by γ rays of ^{137}Cs, then infused 5×10^6 spleen-thymus lymphocytes (ratio 2:1, 0.1 ml) from donor mice through lateral tail veins in 4 h [12]. The Ctrl mice were shame-irradiated for equal time and were infused saline through lateral tail veins. AA mouse model was established successfully after 15 days. The animal experiment was performed in accordance with the guideline for the care and use of laboratory animals of the national institutes of health of China and approved by the Animal Management and Ethics Committee of Tianjin Medical university.

2.2. Cells culture

In the study, the $CD8^+$T cells from mouse spleen were selected as research object. $CD8^+$T cells were isolated by CD8 immunomagnetic beads. And cells were cultured in medium which including RPMI-1640 with 10 % fetal calf serum, 2 mM L-glutamine, penicillin and streptomycin (100 U/ml). $CD8^+$T cells were collected and cultured in the presence of anti-CD3 mAb (5 μg/ml), anti-CD28 mAb (2 μg/ml) and IL-2 (40 ng/ml) in a 37 °C incubator at 95 % humidity and 5 % CO_2.

2.3. Trial grouping

In the experiment, we set three cell models that $CD8^+$T cells were isolated from normal mice and AA model mice, including Ctrl cells group (Ctrl), AA model mice cells group [1], *Tsc2*$^-$ transfection AA cells group (*Tsc2*$^-$). To explore the canonical autophagy pathway, we divided into six groups, NC, AA, AA + DNS, AA + CsA, AA + ISC and AA + RAPA, furthermore, the RAPA, mTORC1

inhibitor, was set as positive Ctrl group. For exploring the non-canonical autophagy pathway, high activity of mTORC1 cell model was built by transfection *Tsc2* of $CD8^+$T cells in AA mice. Therefore, cells were grouped in NC, AA, *Tsc2*$^-$AA, *Tsc2*$^-$AA + DNS, *Tsc2*$^-$AA + CsA, *Tsc2*$^-$AA + ISC and *Tsc2*$^-$AA + C646, furthermore, the p300 inhibitor was set as positive Ctrl group. Each group included 3 mice according to the basis of the previous research of the group.

2.4. Cells transfection

We conducted subsequent experiments by transfecting *Tsc2* gene to achieve high activity of mTORC1 [13]. According to the reagent manufacturer's instructions, transfection was performed when the cell density reached 80 %. Transfection mixtures (100 μl/well) included 5 μl RNA oligo, 50 μl medium and 8 μl siRNA transfection reagent. Mixed them completely and stood at room temperature for 20 min. Next the transfection mixtures were added into cell culture plate, then, cells were incubated at 37 °C, after 6 h the old medium was discarded. To verify the transfection efficiency, mRNA expression was detected 24 h later. Transfection reagents and siRNA used were compound by Gene Pharma company. The gene sequence can be seen in the Supplementary Information Table 1.

2.5. Real-time qPCR

Total RNA was extracted by Trizol and dissolved in DEPC water. After, the solution was diluted 100 times, the wavelength at 260–280 nm was measured by spectrophotometer to calculate the RNA concentration, and then reverse transcription was performed. Subsequently, RT-PCR reaction was performed on Roche LightCycler480II real-time fluorescence quantitative PCR instrument, using primers *Tsc2* and β-actin (Sigma), specific sequences are shown in the Supplementary Information Table 1. We used β-actin as control gene and the data were analyzed by the ΔΔCT method.

2.6. Cell proliferation assay

We used carboxyfluorescein succinimidyl ester (CFSE) to examine cell proliferation. Firstly, CFDA, SE dyeing solution was prepared according to the CFSE kit instructions. Then cells were cultured at a density of 2×10^5 cells/well, cells suspension was mixed with equal CFSE solution and cells were incubated at 37 °C for 10 min in the dark. The reaction was terminated by adding complete medium preheated at 37 °C. Last cells were centrifugated at 300 g for 5 min, and repeated washing. After normal culture, cells were collected at appropriate time and cell proliferation was assessed by flow cytometry.

2.7. CCK-8 assay

We used the CCK-8 to examine drugs concentration. Firstly, cells were isolated after micro beads separation and incubated at a density of 3×10^6 cells/well in 96-well plate for 24 h. Drugs were added in different groups and each sample was set to repeat detection three times. Then, the complete medium was discarded and replaced with 100 μl drug-containing medium at different concentrations so that the final concentrations were 0, 1.25, 2.5, 3.75, 5 μM for the DNS group, 0, 1.25, 2.5, 3.75, 5 μM for the CsA group, 0, 5, 10, 15, and 20 μM for the C646 group and 5, 10, 50, 100, 1000 nM for the RAPA group. Lastly, after intervention for 24 h or 48 h, 10 μl CCK-8 reagent was added to each well and incubated at 37 °C for 4 h, and then the absorbance at 450 nm was detected immediately by enzyme standardization instrument, the standard curve was drowned, and the cell survival rate was calculated. These stock solution of drugs was prepared by dimethyl sulfoxide (DMSO). The final concentration of DMSO in the drug working solution in the cells was $<$0.01 %. DMSO of 0.01 % was used as a vehicle control in all cell culture assays.

2.8. MDC dyeing experiment

After culturing 24 h, Centrifuged and collected cells, added 1 ml MDC staining solution per 1×10^6 cells, resuspended and incubated for 30 min at 37 °C and away from light. After centrifugation, the supernatant was discarded, and 1 ml Assay Buffer was added, resuspended and washed 3 times in total. Then we prepared the cell slides and draw a circle on the glass slides with an immunohistochemistry pen, added 1–2 drops of cell suspension to the center of the circle, covered the slide and sealed the slide with slide mounting medium. The prepared cell slides were properly dried and immediately put into the scanner. The excitation wavelength of 335 nm and emission wavelength of 512 nm were used for fluorescence detection and images were collected. Last, the fluorescence images were observed by three different experimenters, they observed randomly ten selected fields of each smear. The number of autophagosomes which emitted green color of fluorescence in the field of view was counted.

2.9. Apoptosis assay

The cells were collected by centrifuged, washed by PBS for twice and were suspended in 100 μl PBS, 5 μl Annexin-V in combination with 10 μl PI (propidine iodide) were used to detect apoptosis. Next, cells were incubated at room temperature for 15 min in the dark. Lastly, 100 μl PBS was added, images were captured by using flow cytometry instrument to analyze results that early and late apoptotic cells.

2.10. Flow cytometry

Cells were collected by centrifugation at 300*g* for 10 min and washed by PBS three times. Then cells were suspended by 100 μl PBS, according to the experimental requirement, negative tube and single stain tube were reserved and stained with the appropriate mAbs or isotype matched Igs (negative controls) for 30 min at 4 °C away from the light. After staining, the cells were fixed in 1 ml 4 % w/v paraformaldehyde for 30 min. After the cells were washed three times, the prepared samples were detected by flow cytometry.

2.11. Western blot

The total cells protein was extracted by previously prepared protein lysis solution including RIPA, PMSF and phosphatase inhibitor at 100:1:1. All processes should be conducted on the ice. The bicinchoninic acid (BCA) kit was used for protein quantitative analysis, and the protein concentration of each sample was calculated by enzyme standardization instrument at the wavelength of 562 nm. Then each sample protein was quantified and subjected to SDS-PAGE electrophoresis. After protein were transferred to PVDF membranes, following membranes were blocked with Tween 20 (TBST) containing 5 % skim milk for 1 h. The membranes were washed by TBST and incubated with various primary antibodies overnight at 4 °C. After washed three times in TBST, membranes were incubated with secondary antibody at room temperature for 1 h and washed. The membranes were immersed in the configured luminescent solution for 2–3 min and put into a chemiluminescent gel imaging system. For quantifying protein expression, all blots were scanned, and the signal densities were measured using NIH ImageJ software.

2.12. Co-immunoprecipitation

The extraction of total cells protein was same as Western blot, used BCA assay to quantify the input group's protein. The protein A/G-agarose were previously washed by PBS, then were suspended in mixed protein-antibody dilution. They were incubated on suspension instrument overnight at 4 °C. After incubating overnight, they were washed three times with PBS, added 1 × SDS buffer solution and total protein was denatured by boiling at 95 °C for 10 min. Then we used SDS-PAGE electrophoresis and western blotting to analyze Co-IPs.

2.13. ELISA

By using multiple ELISA kit to quantify the cytokine secretion levels in culture supernatants. According to the reagent manufacturer's instructions, at the end, absorbance was measured with an enzyme marker. Above these procedures are wet lab in the vitro. This study is divided into two parts as dry lab (*in silico* studies) and wet lab (in vitro studies) [14].

2.14. In silico docking simulation to explain the inhibition mechanism (dry lab)

Silico docking simulation was utilized to help to explain the mechanism of interaction between p300-CsA, p300-DNS, mTOR-CsA and mTOR-DNS. Firstly, 3D structures models of p300 and mTOR were set up using homology models. Then, autodock software (version 4.2) was used to dock CsA and DNS into the activity cavity of p300 and mTOR isoforms. The non-polar hydrogen atoms of P300 and mTOR were merged. After, the grid box was generated with 60 × 60 × 60 in X, Y and Z coordinate and thus to cover the entire ligand-binding site. Lamarckian Genetic Algorithm (LGA) method was utilized to process molecular docking for the binding of CsA, DNS and p300, mTOR. Finally, hydrogen bonds and hydrophobic contacts were analyzed to reveal the best conformation for interactions between CsA, DNS and P300, mTOR isoforms.

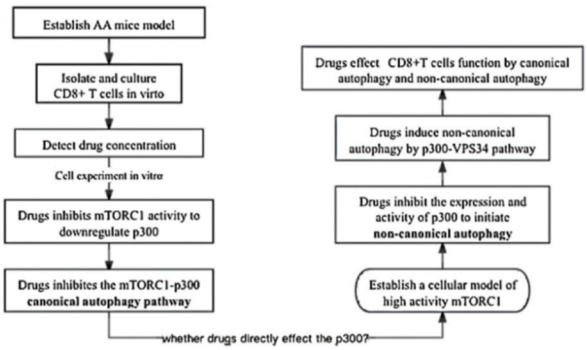

Fig. 1. Flow chat.

2.15. Statistical analysis

The statistical analysis was completed by using GraphPad Prism 8.0 software, starting with a normality test and chi-squared test. The T-test was used to compare data between two groups. A one-way or two-way analysis of variance was used to compare data between multiple groups. The data of the experiment were presented as mean ± standard error (±SEM), $P < 0.05$ means the difference was statistically significant.

2.16. Flow chat

The below is a flow chart to show all the procedures done within the present manuscript in Fig. 1.

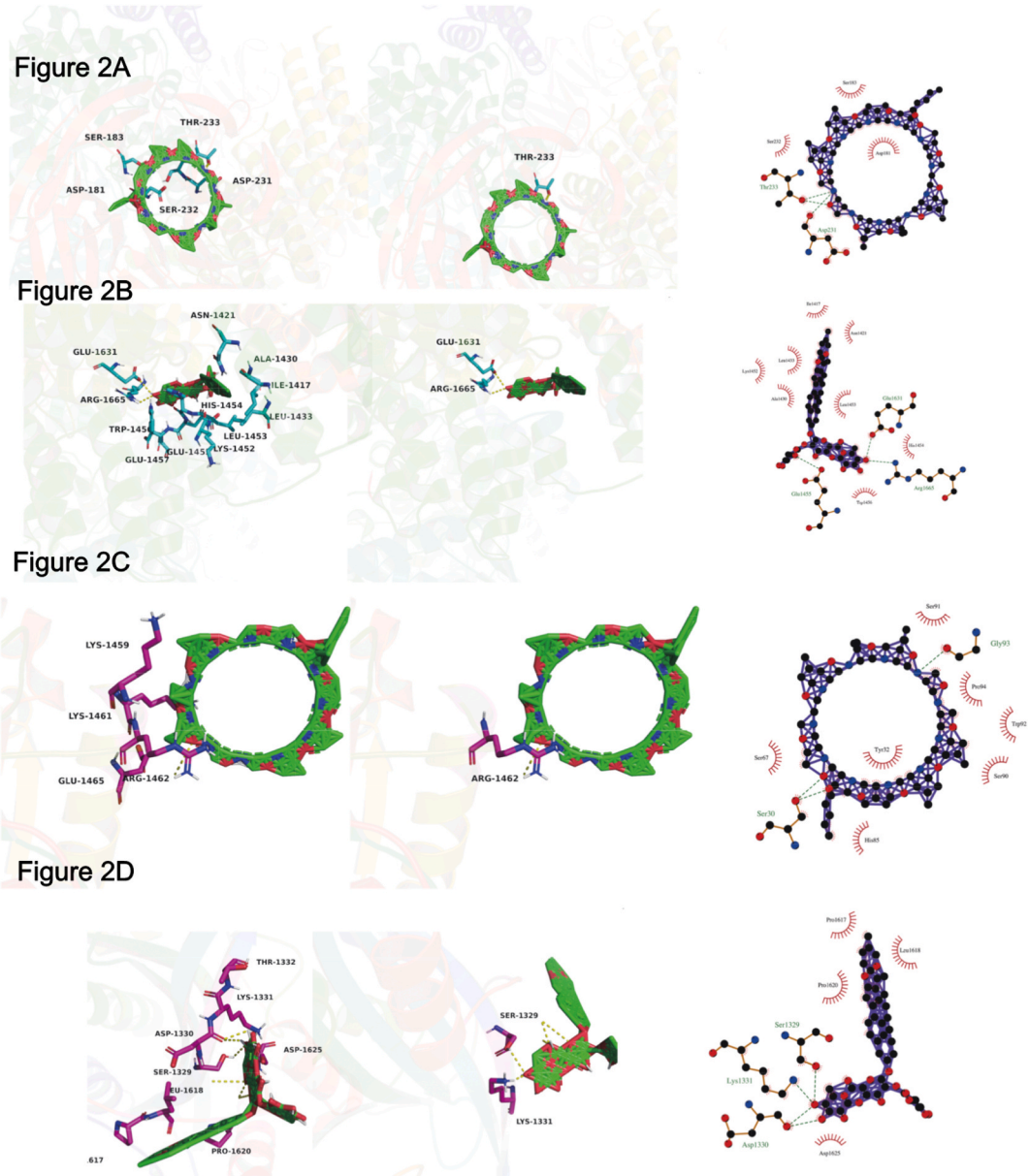

Fig. 2. Prediction of the interaction between ISC (DNS, CsA) and mTOR, p300 protein. (**A**) CsA formed 3 hydrogen bonds and CsA forms the hydrophobic interactions with mTOR. (**B**) DNS formed 3 hydrogen bonds and DNS forms the hydrophobic interactions with mTOR. (**C**) CsA formed 3 hydrogen bonds and CsA forms the hydrophobic interactions with p300. (**D**) DNS formed 4 hydrogen bonds and DNS forms the hydrophobic interactions with p300.

3. Results

3.1. The proliferation and activation of $CD8^+$T cells in vitro

The $CD8^+$T cells from spleen lymphocytes purified by immunomagnetic beads sorting showed a high purity and positive rate. Generally, the results analysis showed that >95 % of $CD8^+$T cells were positive for under PE staining (Supplementary Information Fig. 1A). $CD8^+$T cells were cultured in the medium including anti-CD3 mAb (5 μg/ml), anti-CD28 mAb (2 μg/ml) and IL-2 (40 ng/ml) for 5 days. Then cells were observed under microscope (40× field), and the clump and aggregate phenomenon were found, which was considered as the successful activation. Next, it was decided used CFSE staining assay to detect the proliferation of $CD8^+$T cells in vitro (Supplementary Information Fig. 1B). Using the specific mTORC1 inhibitor RAPA and the CsA as the positive control group treatment. After CCK-8 assays, the result determined the optimal drug concentration respectively were 2.5 μM for DNS, 1.25 μM for CsA, the optimal concentration of ISC was 2.5 μM DNS combination 1.25 μM CsA, 100 nM for RAPA and 15 μM for C646 (Supplementary Information Fig. 2). These results in this section will allow further experiments to be conducted.

3.2. In silico docking results

In silico docking simulation was utilized to explain the mechanism why CsA and DNS could inhibit the activities of mTORC1 and p300. With this method, the binding free energy and the active site could be solved, and the structure-activity relationship for the inhibition capability of CsA and DNS towards mTORC1 and p300 could be tested. Molecular docking assays revealed that CsA may bind to mTOR and p300, DNS also bind to these two proteins. In the binding site of CsA and mTOR, CsA forms three hydrogen bonds with Thr 233 and Asp 231, and hydrophobic interactions with Ser 232, Ser 183, Asp 181 (Fig. 2A). In the binding site of DNS and mTOR, DNS forms three hydrogen bond with Glu 1455 and Glu 1631, Arg 1665, and hydrophobic interactions with Ile 1417, Asn 1421, Lys 1452, Leu 1433, Ala 1430, Leu 1453, His 1454, Trp 1456 (Fig. 2B). Besides, the binding free energy of DNS and CsA with mTOR were −8.92, −10.24 kcal/mol, respectively. In the binding site of CsA and p300, CsA forms three hydrogen bonds with Gly 93, Ser 30 and hydrophobic interactions with Ser 91, Ser 67, Ser 90, Pro 94, Trp 92, His 85, Try 32 (Fig. 2C). In the binding site of DNS and p300, DNS forms four hydrogen bond with Ser 1329, Lys 1331, Asp 1330 and hydrophobic interactions with Pro 1617, Leu 1618, Pro 1620, Asp 1625 (Fig. 2D). In additional, the binding free energy of DNS and CsA with p300 were −12.48, −11.04 kcal/mol, respectively. Based on

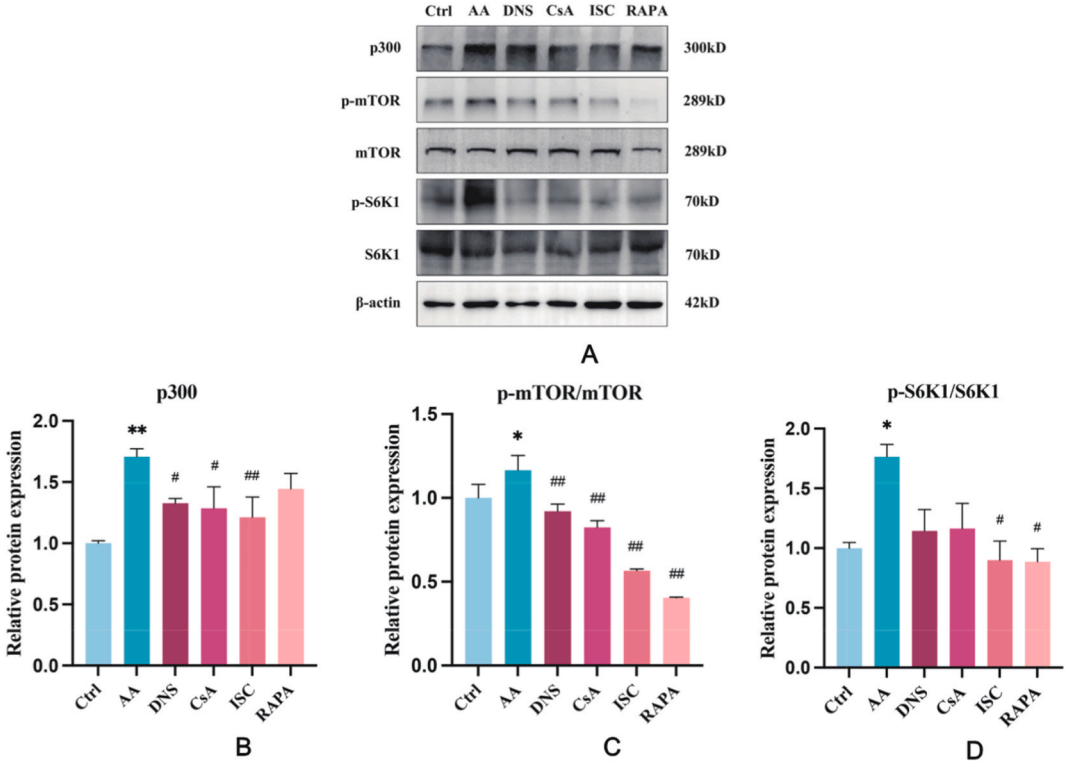

Fig. 3. The inhibition of drugs in the mTORC1-p300 canonical autophagy pathway. (**A**) Expression of *p*-mTOR/mTOR, p300 and p-S6K1/S6K1 in each group. (**B**) The relative protein expression of p300. (**C**) The relative protein expression of *p*-mTOR/mTOR. (**D**) The relative protein expression of p-S6K1/S6K1. (**E**) The combination between p300 and LC3 protein in each group. Co-immunoprecipitation of acetylated protein with LC3 and relative expression of acetylated protein in each group. (**F**) The acetylation level of LC3 in each group. *P < 0.05, **P < 0.01 vs. group Ctrl; $^{\#}$P < 0.05, $^{\#\#}$P < 0.01 vs. group AA. The full, non-adjusted images were obtained in the SI (Repeat gels of Fig. 3 and 4).

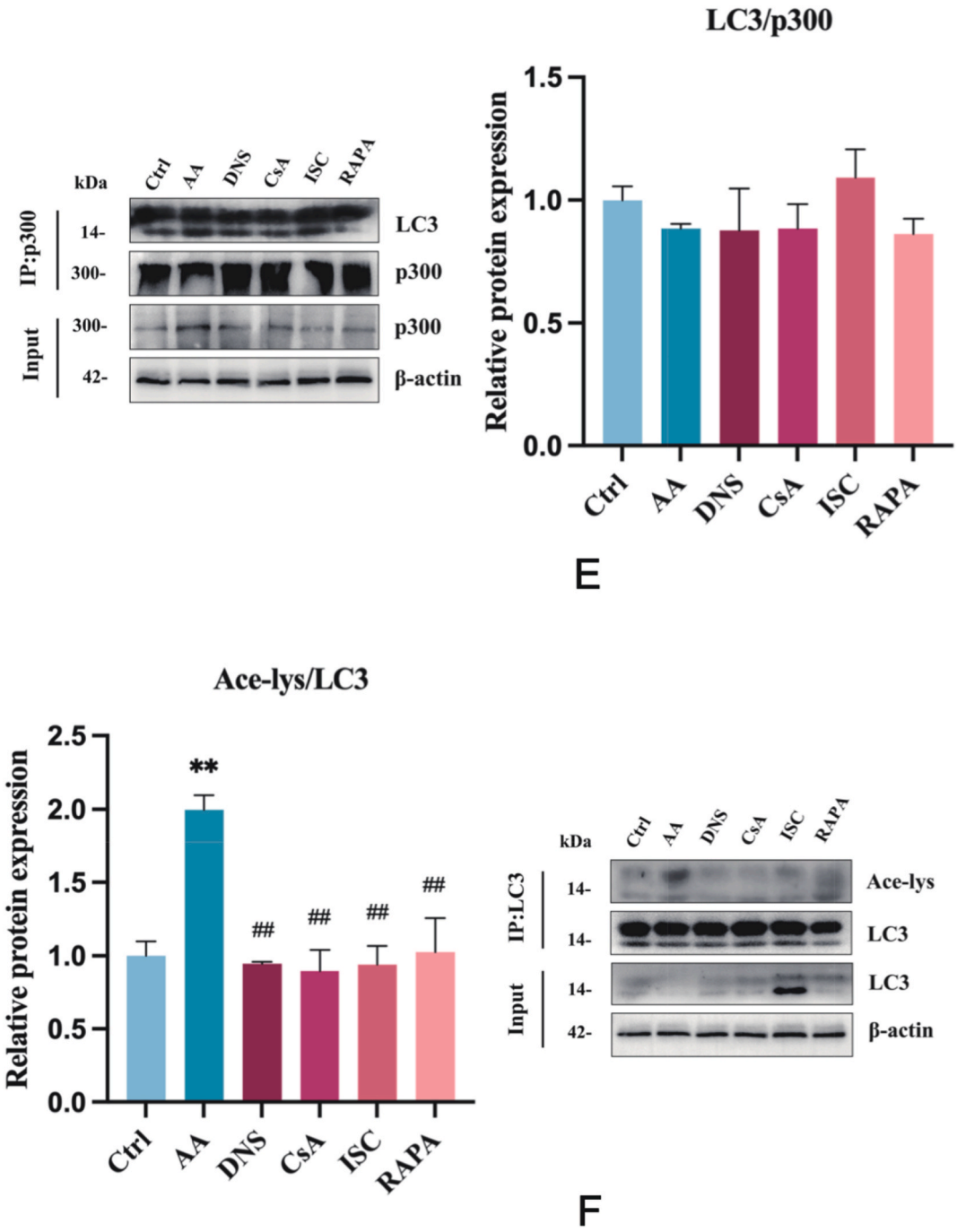

Fig. 3. (*continued*).

the above results, it can conclude that hydrogen bonds contributed to the strongly inhibitory capability of DNS and CsA, and hydrophobic contacts contributed to the strongly inhibitory capability of DNS and CsA to mTORC1 and p300.

3.3. ISC inhibits mTORC1 activity to downregulate p300

The mechanistic target of RAPA is a master regulator of autophagy, mTOR interacts with specific adaptor proteins and forms the mTOR complex 1 (mTORC1) which is a distinct macromolecular complex [15]. p300 is a phosphorylation substrate of mTORC1, and this phosphorylation is necessary for the function of p300 in inhibiting autophagy and activating transcription [8]. To investigate the importance of ISC in regulating mTORC1-p300, it was decided first used an assay to examine whether ISC affected mTORC1 expression

and phosphorylation. It was decided that use the expression of phosphorylation mTOR (*p*-mTOR) and the persistent phosphorylation of S6K1 (p-S6K1), the substrate of mTORC1, to represent the activated mTORC1 activity [16]. Using the specific mTORC1 inhibitor RAPA as the positive control group and the normal mice $CD8^+$T cells as controls, it was decided found that treatment of cells with DNS, CsA, ISC and the RAPA all reduced the *p*-mTOR, however, the expression of mTOR was unchanged obviously in every group (Fig. 3C). As for anticipation, the phosphorylation of p-S6K1 showed downregulation after DNS, CsA, ISC and RAPA treatment compared with AA group. Noticeably, the decreased *p*-mTOR and p-S6K1 were the most obvious in the ISC group when compared to the DNS or CsA group (Fig. 3D). It showed that ISC inhibition aimed on the mTORC1 activity represented by *p*-mTOR and p-S6K1 rather than mTORC1 expression (Fig. 3A). p300, the substrate of mTORC1, was used to assess the interaction between mTORC1 and p300 by Western blot. mTORC1 activated p300 activity through phosphorylating p300 to further play p300 acetyltransferase activity in regulating cell physiological processes, such as autophagy [8]. It was decided that evaluated p300 activity by assessing the acetylate of its substrate. p300 acetyltransferase regulates autophagy by a number of protein such as LC3, p62 and other proteins [17]. LC3B, an alternative splicing variant of LC3, is the only known mammalian protein present in the autophagosomal membranes and as an autophagosomal marker. Thus, it was decided that illustrated the role of LC3 acetylate in representing p300 activity [18]. Level of LC3 acetylation and p300-LC3 interaction were determined by immunoprecipitation, it was decided that prepared $CD8^+$T cell lysates and assessed whether coimmunoprecipitate endogenous LC3 and p300 in a complex. As demonstrated in Fig. 3E, the reciprocal immunoprecipitation of p300 could coimmunoprecipitate LC3. However, there was no statistical difference between Ctrl group and AA group, similarly, and there was no statistical difference among DNS, CSA, ISC and RAPA groups. It means that drugs unaffected on the combination of p300 and LC3 (Fig. 3E). Under similar conditions, it was decided that detected the change of LC3 acetylation (Fig. 3F). Specifically, when we assessed LC3 expression and its acetylation in $CD8^+$T cells, it noted that acetylate level of LC3 appeared to increase in AA model group whereas decreased in ISC, DNS, CsA and RAPA group. What is important, the decreased acetylation level was more obviously in the ISC group. These findings demonstrated that ISC had the similar effect, like RAPA, inhibiting mTORC1 activity to suppress the p300 activity. Interestingly, not only did ISC inhibit the p300 activity, but also downregulated the expression of p300 (the substrate of mTORC1). The expression of p300 increased in AA model group compared with Ctrl group, nevertheless, it was decided found that the lower expression of p300 demonstrated in DNS, CsA and ISC group than AA group. The decreased expression was obvious in ISC group,

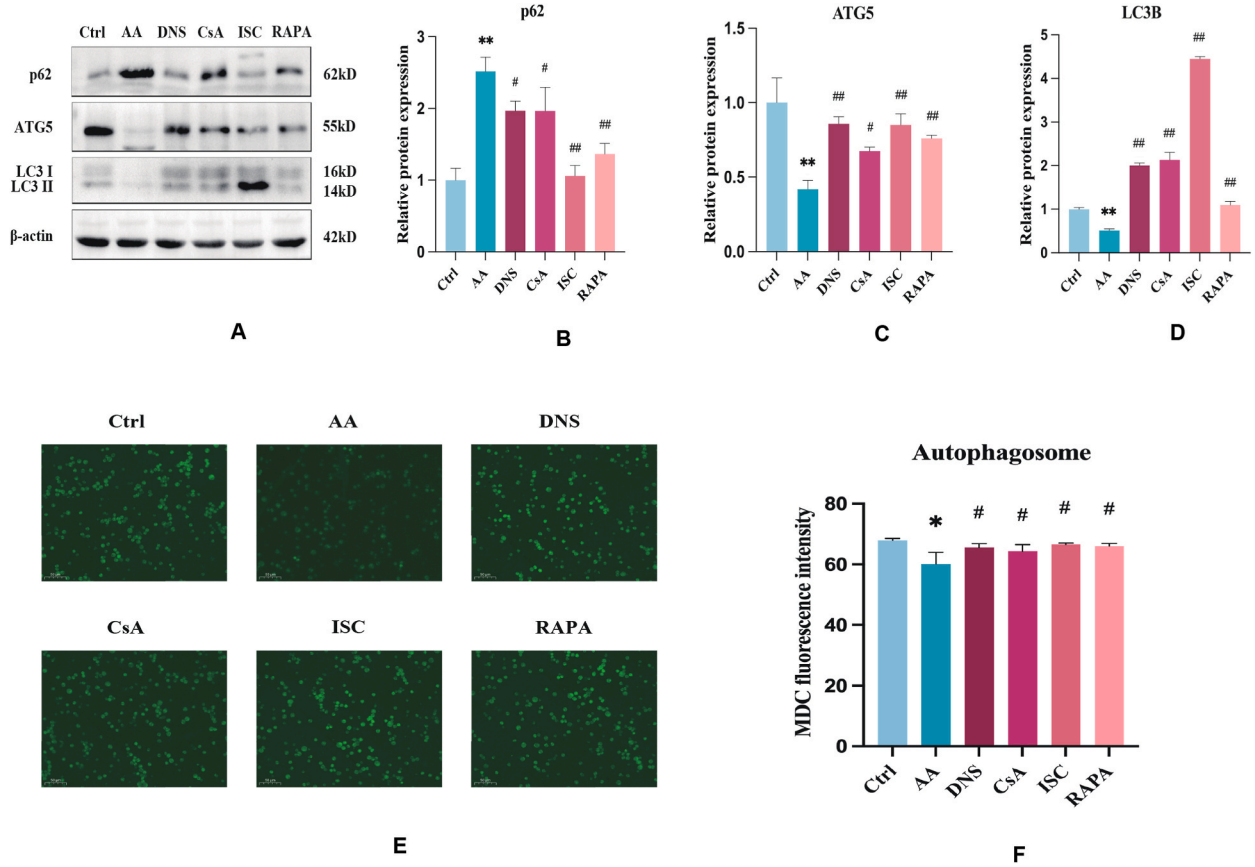

Fig. 4. Autophagy related protein expression in each group of canonical autophagy. (**A**) The expression of p62, ATG5 and LC3 in each group. (**B**) The relative protein expression of p62 in each group. (**C**) The relative expression of ATG5 in each group. (**D**) The relative protein expression of LC3 in each group. (**E**) MDC staining scan results of each group. (**F**) Fluorescence intensity of MDC staining in each group. $^*P < 0.05$, $^{**}P < 0.01$ vs. group Ctrl; $^{\#}P < 0.05$, $^{\#\#}P < 0.01$ vs. group AA. The full, non-adjusted images were obtained in the SI (Repeat gels of Fig. 3 and 4).

but there was quite small decreased in the DNS group and the CsA group. However, the RAPA group unaffected on the expression of p300 (Fig. 3B). It indicated that ISC had the inhibition on the p300 expression, which was different from RAPA. Generally, our findings suggested that high levels of mTORC1 and p300 activity, the mTORC1-p300 axis, played an important role in the AA mechanism. ISC inhibited the mTORC1 activity to suppress p300 activity and downregulated the expression of p300.

3.4. ISC induces canonical autophagy by mTORC1-p300 pathway

The mTORC1-p300 pathway regulates cell canonical autophagy and cell lipogenesis [8]. p300 plays an important role in modulating autophagy-related proteins such as ATG5, ATG7, ATG8, and ATG12 [17]. ATG5, an autophagy-related protein, was demonstrated that its mutation was involved in AA mechanisms and it was critical to prove drug-induced canonical autophagy by assessing the substrate of p300 [19]. One useful marker for autophagy induction was the conversion of LC3-I to LC3-II, and the other was p62 bodies that were degraded by autophagy via LC3 [20]. The first found was that the AA model group cells had significantly higher expression of p62 than the Ctrl group. To address the role of the autophagy pathway in the occurrence of AA, it was decided that analyzed whether inhibiting the critical protein mTORC1 influences the level of autophagy downstream proteins (LC3, ATG5 et al.) in $CD8^{+}$T cells. Obviously, decreased acetylation level was primarily in LC3-I rather than LC3-II, and ISC treatment dramatically increased the expression of LC3-II and even more had highly enhanced compared with RAPA group (Fig. 4A). Meanwhile, our data showed that the expression of p62, substrate for LC3, decreased after treatment with ISC, further supporting the notion that ISC induces autophagic flux. Additionally, the autophagy protein ATG5 also increased after treatment. As an inhibitor of mTORC1, the RAPA group had an obvious change compared with AA model group, as well as these drug treatment groups had a similar trend with RAPA group. After drugs intervening, especially in the ISC group, ATG5 showed obvious increase compared with DNS group and CsA group (Fig. 4B–D). Taken together, these data verified that AA mechanism had the deficiency of autophagy and ISC promoted autophagy by inhibiting mTORC1. To further determine whether drugs aimed at inducing canonical autophagy were effective, the cells were subsequently stained with MDC to observe autophagosomes under a fluorescence microscope. The Ctrl group had lower numbers of

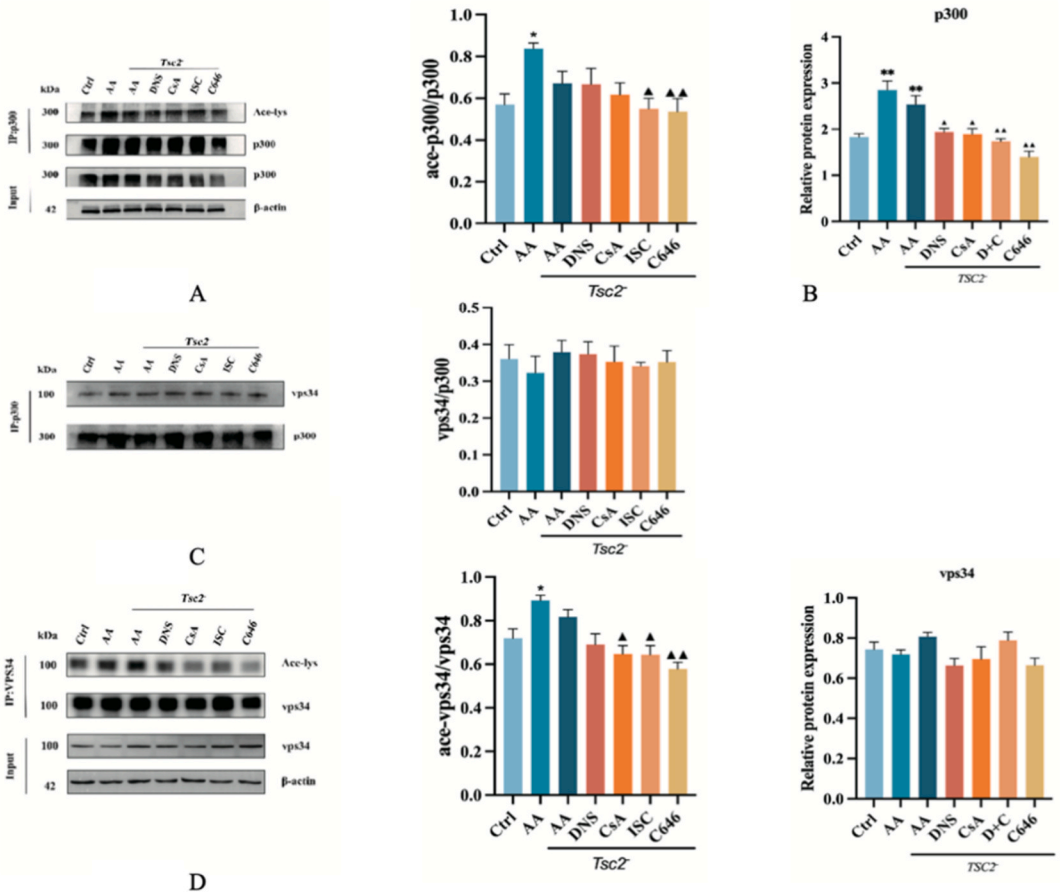

Fig. 5. The inhibition of drugs in the p300-VPS34 non-canonical autophagy pathway. (**A**) Expression of p300 protein and its autoacetylation level in each group. (**B**) The relative expression and acetylation level of p300 protein in each group. (**C**) CO-IP was used to detect the binding of p300 and vps34 proteins in each group. (**D**) The relative expression and acetylation level of vps34 protein in each group. $^{*}P < 0.05$, $^{**}P < 0.01$ vs. group Ctrl; $^{▲}P < 0.05$, $^{▲▲}P < 0.01$ vs. group *Tsc2*$^{-}$AA. The full, non-adjusted images were obtained in the SI (Repeat gels of Fig. 5 and 6).

autophagosomes staining than the AA model group. Furthermore, MDC staining revealed that drug treatment stimulated autophagy in CD8+T cells, as evidenced by the increased MDC positive ratio. The changes in autophagy were reflected by MDC staining. Our statistical results presented ISC stimulated more autophagosomes, relative to the number of autophagosomes that DNS and CsA stimulated (Fig. 4E–F). The results suggested that there is a decreased acetyltransferase activity of p300 with drugs inhibiting especially the suppression by ISC. All in all, it suggested that ISC, DNS, CsA treatment is associated with an increase in autophagic flux as a result of a decrease in acetyltransferase p300 and acetylation of autophagic marker protein LC3 in $CD8^{+}$T cells.

3.5. ISC inhibits p300 expression and activity directly

In our previous study, an interesting finding was that not only did ISC inhibit p300 activity, but also decreased the p300 expression, which was different from RAPA. Thereby It was decided investigated the ISC treatment whether plays a critical role in regulating p300 without mTORC1 mediation directly, which means promotes non-canonical autophagy. Non-canonical autophagy is unlike in canonical autophagy, and its initiation can bypass the AMPK–mTORC1–ULK1 circuit [21]. A previous study illustrated mTORC1 is a key downstream target of *Tsc2* to mediate the cellular response, and *Tsc2* is a suppressor of mTORC1 to inhibit its activity and downstream signaling [22]. Knockdown the mTOR is the usual way to research non-canonical autophagy. To study the function of p300 on the non-canonical autophagy pathway, a cellular model of high activity mTORC1 was established by transfecting *Tsc2* siRNA in $CD8^{+}$T cells, which as a key player in regulation of the common mTOR pathway of protein synthesis (here after referred to as si-*Tsc2* or *Tsc2*$^{-}$). *Tsc2*$^{-}$ $CD8^{+}$T cells model establishment was aimed to highly activity mTORC1 to illustrate p300 is essential for non-canonical autophagy. To determine whether p300 activity and expression was affected by experimental drugs (ISC, DNS, CsA and C646, a p300 inhibitor was used as the positive group). Western blot analysis confirmed that the protein expression of p300 was upregulated in AA model and *Tsc2*$^{-}$ model cells compared with Ctrl group cells, and the interesting thing was *Tsc2* transfection had little influence on the expression of p300. Meanwhile, the expression of p300 was decreased in all drug treatment groups especially obvious in the ISC group (Fig. 5B). In the experiment, the activity of p300 was represented by its substrate or itself autoacetylation [17]. In addition, the results of co-IPs showed obviously increase of p300 itself acetylation in AA group and *Tsc2*$^{-}$ group comparing with Ctrl group. However, compared with *Tsc2*$^{-}$ group, the acetylation of p300 was downregulated in ISC, DNS and CsA group and p300 activity was dramatically inhibited by ISC treatment (Fig. 5B). All in all, the significant differences in every group demonstrated ISC, DNS and CsA inhibits the expression and activity of p300 to initiate non-canonical autophagy even though the mTORC1 had high activity which is the inhibiting signal of autophagy.

3.6. ISC induces non-canonical autophagy by p300-VPS34 pathway

Acetylation by p300 suppressed VPS34 lipid kinase activity, and this acetylation/deacetylation-based mechanism by the p300-VPS34 pathway was involved in the initiation of autophagy, and VPS34 activation requires VPS34 deacetylation [23]. Our subsequent multiple analyses confirmed that VPS34 is a potential substrate of p300 during autophagy. It was decided to examine whether and how p300 expression regulates VPS34 acetylation in autophagy. An immunoprecipitation analysis revealed the difference of bond between VPS34 and p300 in $CD8^{+}$T cells and *Tsc2*$^{-}$ $CD8^{+}$T cells following treatment with drugs (DNS, CsA, ISC and C646) was not significant, in comparison with the AA model group (Fig. 5C). As well as there was no remarkable difference in Ctrl group and AA model group. However, the changes in the VPS34 acetylation had a correlation with the protein activity of p300. Functional assays demonstrated that drugs failed to affect bond between VPS34 and p300 but inhibited the acetylation of VPS34. Western blot analysis showed that the acetylation of VPS34 increased in AA model group and *Tsc2*$^{-}$ AA model group, whereas the acetylation was reduced in every drug administration group compared with the Ctrl group and the deacetylation trend was most obvious in the ISC group compared with DNS and CsA group (Fig. 5D), suggesting that the occurrence of the VPS34 deacetylation in drug group cell came from the inhibition of p300. Altogether, these findings not only supported a critical role for p300 inhibitors in promoting the deacetylation of VPS34, but also explained why only selectively regulated VPS34 acetylation rather than combination of both, based on p300-VPS34 pathway.

It is essential to identify protein expression of autophagic occurrence in order to unravel the mechanism of the drug inhibited p300 induce non-canonical autophagy phenomenon. Based on previous autophagy occurs relative protein findings [20,24], several methods were used in the experiment to further test the autophagy flux. It demonstrated that the expression of downstream autophagy-related proteins (ATG5 and LC3) in the AA model and *Tsc2*$^{-}$AA groups were significantly lower than that in the Ctrl group. On the contrary, the expression of p62 was increased in two AA model groups, suggesting that a decreased autophagic flux appeared in $CD8^{+}$T cells with the occurs of AA mechanisms. The increase in autophagic flux was associated to the use of drugs (ISC, CsA and DNS) inhibited the expression and activity of p300 in $CD8^{+}$T cells, resulting in VPS34 deacetylation. Furthermore, increased LC3 expression was more prevalent in LC3-II than LC3-I. Strikingly, the analysis revealed that the ISC group had the most highly expression of LC3 than the DNS and CsA groups even than the p300 inhibitor (C646) group. For the expression of ATG5, ISC group was the only group with statistical difference among the four treatment groups compared with *Tsc2*$^{-}$ group. As same as degradation of p62, the ISC group showed dramatically decrease than another drug groups (Fig. 6). Together, our Western blot results suggested that an increase in autophagic flux was related to the use of medications due to a mechanism involving the p300-VPS34 pathway and the LC3-p62 pathway in the onset of autophagy.

To study whether ISC, CsA and DNS inhibited the expression and activity of p300 to onset non-canonical autophagy, MDC staining was utilized to label autophagosomes in $CD8^{+}$T cells. And the numbers of autophagosomes decreased significantly in the AA model group compared with the Ctrl group, and the amount of autophagosomes was at least partially reversed in the group of ISC, DNS, and

CsA compared with the AA model group and TSC^{-}AA group. Apart from C646 group, the ISC group had the second amount of autophagosomes with the statistical difference, which demonstrated that the autophagy was induced after drug treatment and autophagy deficiency led by AA can be reversed by p300 inhibitor (ISC, DNS and CsA) treatment (Fig. 6C–D).

3.7. ISC effected CD8^{+}T cells function by canonical autophagy and non-canonical autophagy

Next it was determined to explore what is the role of autophagy in AA CD8^{+}T cells. Investigation of CD8^{+}T cells surface activation markers, CD44, CD25 and CD69 expression were detected by flow cytometry (Fig. 7A–B). It can be seen CD25 and CD69 significantly increased and CD44 markedly decreased in AA group and *Tsc2*$^{-}$ group compared with Ctrl group, nevertheless, from DNS-treated, CsA-treated and ISC-treated cells, the CD25 and CD69 expression were down regulated and the CD44 expression level was reduced by the drugs. Furthermore, the ISC group showed more lower expression in the activation markers (CD25, CD69, CD44) than the DNS and CsA groups and had the statistical difference, suggesting that the ISC inhibited the activation of CD8^{+}T cells (Fig. 7D–E).

Previous research reported that abnormal activating CD8+T cells play a role in promoting the immune pathogenesis of SAA and correlate with disease severity [8]. Furthermore, the function of CD8^{+}T cells were evaluated by the expression of IFN-γ, perforin and granzyme B. After Elisa assays, comparing with the AA and *Tsc2*$^{-}$ groups, the results showed a significantly decreased trend in the drug-treated groups. Which is worthy to note is that ISC treatment had the most distinctly effect on CD8^{+}T cell function (Supplementary Information Table 2). Additionally, the C646 group, which is inhibitor of p300 and the RAPA group (mTORC1 inhibitor), was also decreased the expression of IFN-γ, perforin and granzyme B, compared with the *Tsc2*$^{-}$ and AA group (Fig. 7C–F), suggesting that inhibiting CD8^{+}T cells activation and function is critical to the CD8^{+}T cells hyperfunction mediated immune unbalance of AA mechanism. Taken together, these data suggested that the hyperfunction of CD8^{+}T cells induced by autophagy deficiency, via ISC treatment that mTORC1 inhibition mediated canonical autophagy and p300 inhibition mediated non-canonical autophagy, was reversed in AA (Fig. 8A and B).

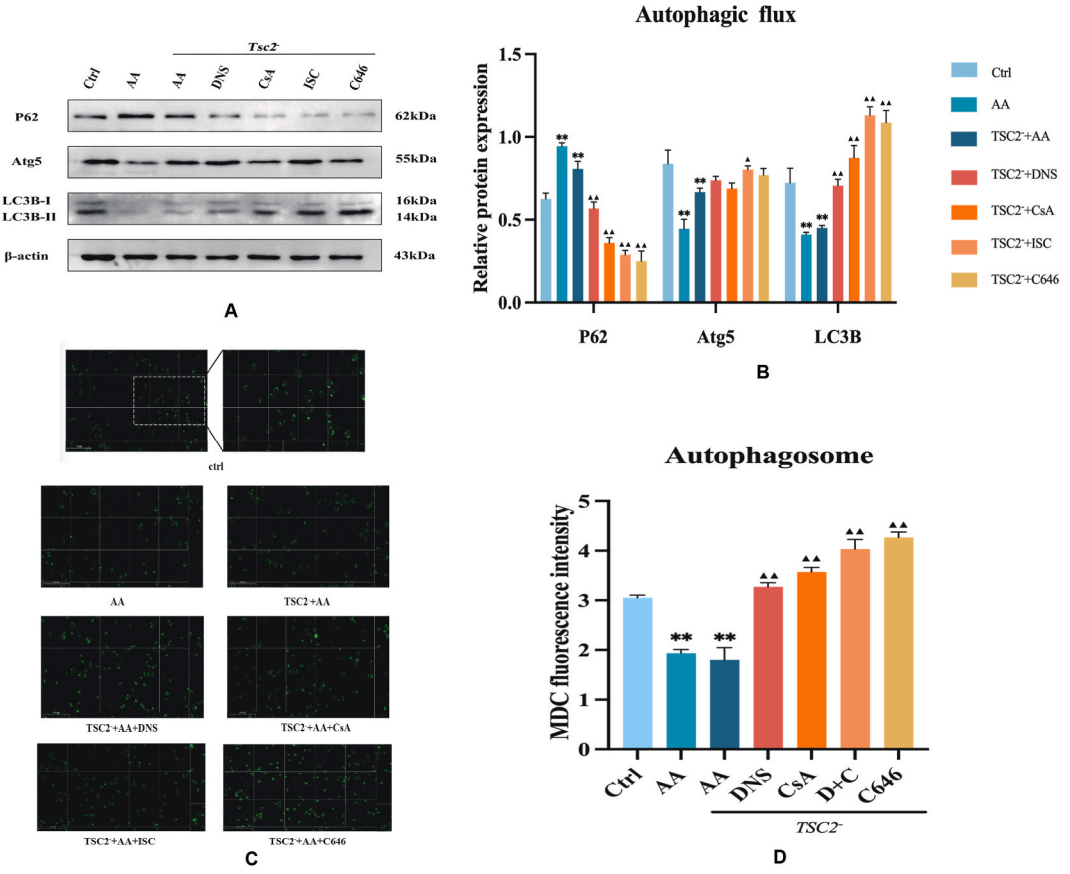

Fig. 6. Autophagy related protein expression in each group of non-canonical autophagy. (**A**) The expression of p62, ATG5 and LC3 in each group. (**B**) The relative protein expression of p62, Atg5 and LC3 in each group. (**C**) Fluorescence intensity of MDC staining in each group. **P* < 0.05, ***P* < 0.01 vs. group Ctrl; ▲*P* < 0.05, ▲▲*P* < 0.01 vs. group *Tsc2*$^{-}$AA. The full, non-adjusted images were obtained in the SI (Repeat gels of Fig. 5 and 6).

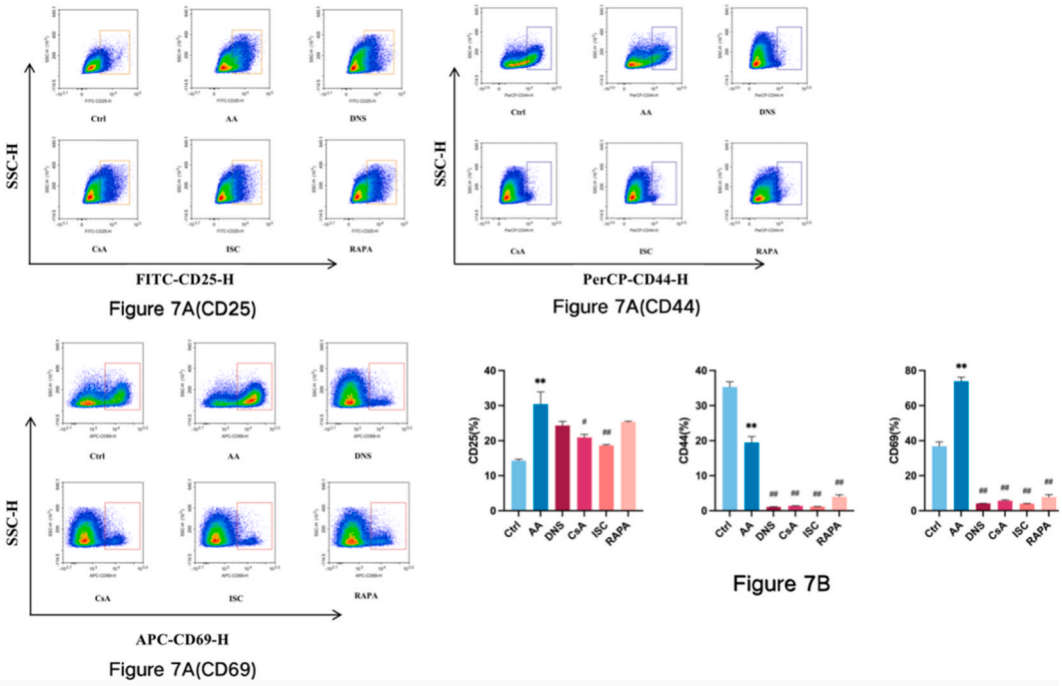

Fig. 7. The activity and function of CD8$^+$T cell in each group of canonical/non-canonical autophagy. (**A**) The expression of CD25, CD44 and CD69 in canonical autophagy. (**B**) The expression levels of CD8$^+$T cell surface activated molecules in each group of canonical autophagy. (**C**) The level of IFN-γ, perforin and GZMS-B cytokines in each group of canonical autophagy. (**D**) The expression of CD25, CD44 and CD69 in non-canonical autophagy. (**E**) The expression levels of CD8$^+$T cell surface activated molecules in each group. (**F**) The level of IFN-γ, perforin and GZMS-B cytokines in each group of non-canonical autophagy. $^*P < 0.05$, $^{**}P < 0.01$ vs. group Ctrl; $^{\#}P < 0.05$, $^{\#\#}P < 0.01$ vs. group AA; $^{\blacktriangle}P < 0.05$, $^{\blacktriangle\blacktriangle}P < 0.01$ vs. group *Tsc2*$^-$AA.

4. Discussion

Autophagy, a conventional cellular progress which the cytoplasmic vesicles, were degraded through delivering to the lysosome and played a pivotal role on maintaining the cells homeostasis and survival [25]. It was regulated under the especially physiological or pathological stimulations such as starved or infection [26,27]. Thereby, identifying the accurate functions of autophagy in different disease backgrounds to determine whether inhibit or induce the autophagy is essential to therapy the specific disease. More and more evidence revealed the change of autophagy in body health and diseases progress. Regarding the cancers, autophagy seems to have the two-sided mechanism that it prevents the cancer cells growth at the outset; however, it was utilized to cytoprotect cancer cells during the cancer processing [28,29]. Autophagy also works on the immunoregulation, ageing and longevity [25]. Autophagy was divided into three classes: macroautophagy, selective autophagy and chaperone-mediated autophagy. Macroautophagy is the best comprehensively autophagy class [30]. Generally, our study was mainly surrounded by the macroautophagy (hereafter referred to as autophagy) and focused on the role of autophagy in AA mechanism.

AA is a bone marrow failure syndrome. The main characteristics of AA were peripheral pancytopenia and bone marrow hypoplasia [31]. However, the AA mechanism was complex and unclear. Recently, it is believed that bone marrow failure caused by abnormal activation and hyperfunction of T lymphocytes is dominant in AA. In addition, the differentiation of helper T cell subset, Th17 and Treg immunosuppressive dysfunction, dendritic cells, macrophages dysfunction and genetic background are all involved in the pathogenesis of AA [32]. CD8$^+$T cells are the main effector cells of the adaptive immune response and play a critical role in AA. The abnormally activated CD8$^+$T cells release perforin, granzyme B with cytotoxic functions upon antigen stimulation or induce apoptosis in HSPCs through Fas-Fas ligand binding and HSPCs were killed indirectly by secreting TNF-α and IFN-γ. The mechanism of activated CD8$^+$T cells in AA has been extensively investigated that the number of CD8$^+$HLA-DR$^+$T cells increased in the peripheral blood of AA patients and the upregulation of perforin, granzyme B, TNF-β and FasL [33]. The expression of tumor necrosis factor-related apoptosis-inducing ligand (TRAIL) in CD8$^+$T cells of AA patients was negatively correlated with the expression of perforin and granzyme B and the apoptosis of CD8$^+$T cell [34]. One study showed that inducing autophagy improved the overabundance of potassium in the tumor microenvironment by enhancing tumor clearance CD8+T cells [35].

DNS, an important component of dioscorea, has the chemical formula $C_{45}H_{72}O_{16}$ and is structurally related to steroid hormones and several paper documented that DNS is effective in the treatment of coronary artery disease, hypolipidemic, antioxidant, anti-inflammatory and anti-tumor [36]. Our previous studies on the mechanism of DNS for AA treatment found the following effects:

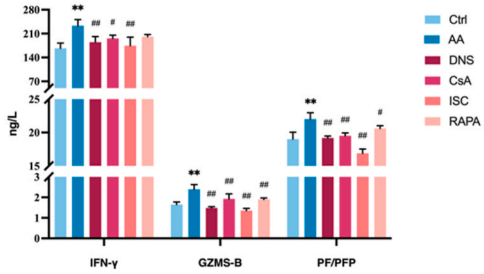

Figure 7C

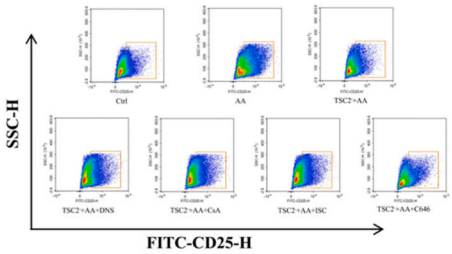

Figure 7D(CD25)

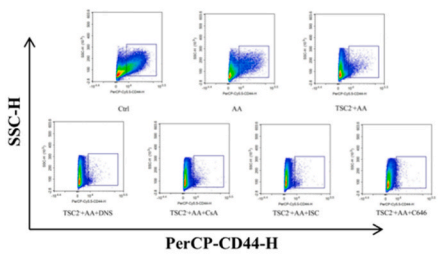

Figure 7D(CD44)

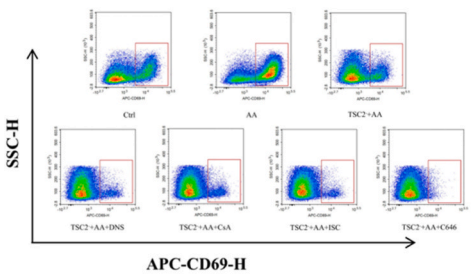

Figure 7D(CD69)

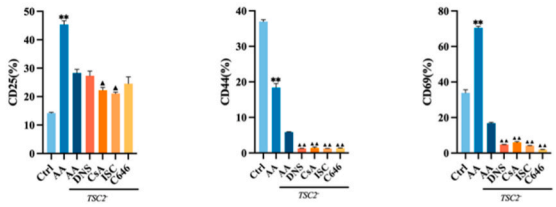

Figure 7E

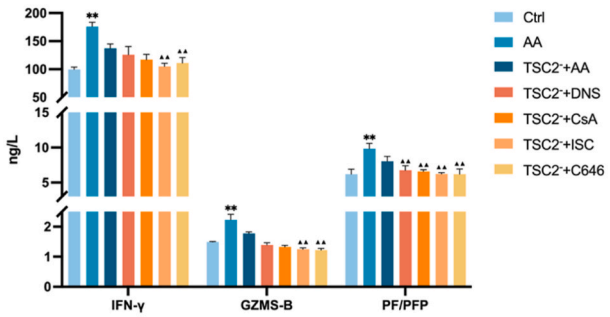

Figure 7F

Fig. 7. (*continued*).

(1) inhibiting effective T cell activity and function, restoring Treg immune tolerance function and the imbalance of bone marrow to recover immune homeostasis [9]; (2) inhibiting bone marrow hematopoietic stem cell apoptosis and promoting bone marrow hematopoiesis [37]; (3) inhibiting bone marrow mesenchymal stem cell adiposity and improving the bone marrow microenvironment [38]. CsA, a type of immunosuppressant, is the clinical first-line immunosuppressive therapy of AA [39]. However, IST is associated

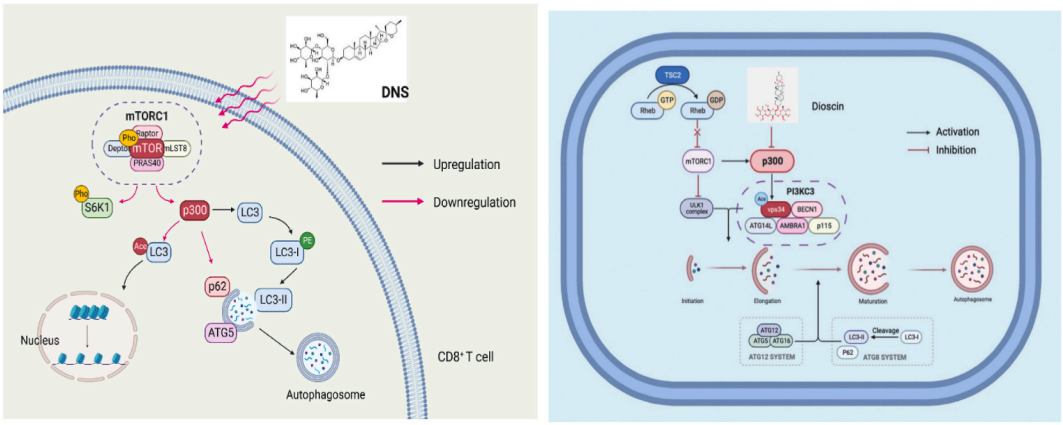

Fig. 8. Diagram of canonical and non-canonical autophagy mechanisms (**A**) The mechanism of DNS induced canonical autophagy. (**B**) The mechanism of DNS induced non-canonical autophagy.

with a high number of side effects and a relapse rate up to 10 %, while nearly 30 % of patients are tolerant to IST. Patients are exposed to repeated dosing and blood infusion dependence for a long time, which seriously threatens both survival and quality of life, hence the importance of exploring new treatment strategy and drug discovery to target the mechanism of AA. In conclusion, even though it was well-known that the DNS and CsA have the immunosuppressive function, however the mechanism of both is unclear. Generally, our study implemented to research the monotherapy (DNS, CsA) and the ISC therapy combining DNS with CsA to further explore the immunosuppressive role to the $CD8^{+}$T cell hyperfunction in AA.

Autophagy was proved that the contribution on the homeostasis of T lymphocyte and autophagic signaling molecules were involved in maintaining this homeostasis progress [30]. The canonical autophagy was controlled mainly by AMPK–mTORC1–ULK1 axis, although many of its direct targets remain unknown, the key breakthrough in this signal pathway is mTORC1, which is essential for autophagy induction [40]. Notably, a latest important finding is mTORC1-dependent phosphorylation of p300 suppresses cell-starvation-induced autophagy and activates cell lipogenesis. In short, p300 is a direct target of mTORC1 [8]. It is an important sparking inspired us to probe the involvement of mTORC1-p300 pathway in the $CD8^{+}$T cells autophagy regulation. In addition, the activity of mTORC1 was represented by itself phosphorylation and its substrate S6K1 phosphorylation level [1]. Meanwhile, p300 is target to several ATG protein such as LC3 (a mammalian homolog of yeast ATG8), ATG5 and ATG7 and these proteins are targeted by p300-mediated acetylation to inhibit the autophagy activity [41]. According to this research, it was determined to detect the canonical autophagy that primarily leading by mTORC1-p300, therefore *p*-mTOR, p-S6K1 and LC3 acetylation were detected, and the results were shown in Fig. 3. A surprising finding was the expression of p300 decreased in the ISC group, however the RAPA as the mTORC1 inhibitor unaffected the p300 expression. At present, there are bottlenecks in the development of drugs in the classical autophagy pathway, such as the low response of sirolimus, the mTOR inhibitor. Based on this unexpected finding, it was proposed whether ISC directly inhibits p300 bypass the mTORC1, which is different from RAPA. Qi, W et al. found that p300/CBP expression in $CD8^{+}$T cells was significantly higher in AA patients and positively correlated with disease severity [6]. Then it was focused on the role of p300 in the autophagy. Protein major epigenetic regulatory mechanism is regulated by histone acetyltransferases (HATs) and histone deacetylases (HDACs). Later, HATs and HDACs were renamed to lysine acetyltransferases (KATs) and lysine deacetylases (KDACs), respectively [42]. It is known that p300 is one of the KATs and regulates gene expression by acetylating histones and other transcription factors [43]. Acetyltransferase p300 (KAT3B) and histidylated SIRT1 are important regulatory enzymes of autophagy and can act to initiate or inhibit autophagy depending on their substrates [44]. For example, BAT3 regulates p300-dependent acetylation of p53 and ATG7 to control autophagy. p300 acetylates the ATG8-PE ubiquitination system to inhibit autophagy [45,46]. mTORC1 phosphorylates p300 carboxy-terminal serine residues and activates their activity, and p300-mediated acetylation further inhibits VPS34 activity thereby suppressing the initiation of canonical and non-canonical autophagy [8,23]. These reports suggest us to explore the non-canonical autophagy that controlled by p300-VPS34 axis. To elucidate the pathogenesis of AA and provide the experimental basis for potential therapeutic targets of ISC, the role of non-canonical autophagy in $CD8^{+}$T cells was further investigated. The complex products produced by the *Tsc2* gene inhibit the phosphorylation of S6K, which is the production of mTOR phosphorylation [22]. *Tsc2* plays a critical role in the mTOR activity. Thus, a cell model with high mTORC1 activity was established by transfecting *Tsc2* RNA in $CD8^{+}$T cells to explicit whether ISC directly initiate non-classical autophagy by inhibiting the activity and expression of p300. C646 as the most effective and potential small molecule p300/CBP inhibitor identified to date [47]. As Fig. 5 shown, ISC had the similar inhibit effect with C646 on the p300, what is different, ISC inhibited the p300 activity and expression. VPS34, the substrate of p300, was obviously deacetylated by ISC and C646. Taken together, ISC has the inhibit effect on the mTORC1-p300 axis and p300-VPS34 axis. Thereby, it was decided to detect the autophagy downstream proteins such as p62, ATG5, LC3 I and LC3 II. ISC decreased p62 expression and upregulated the ATG5, LC3 I and LC3 II. These proteins were detected both of the canonical autophagy and non-canonical autophagy and had the same trend between both of two autophagy pathways as shown in Figs. 4 and 6.

The CTL progenitor (initial $CD8^+$T cells) recognizes the antigenic peptide signal (first signal) through the "MHC I-antigenic peptide-TCR" molecule and binds to CD28 on the surface of the APC to form the second signal, which activates $CD8^+$T cells into the proliferation and differentiation period. Due to the importance of immune system in different organisms, the genes belonging to immune elements, such as ILs, have been studied vigorously [10]. After activation, T cells rapidly secrete IL-2, while the IL-2 receptor α chain (CD25) starts to be expressed after 2 h, forming a heterotrimer with the already constitutively expressed IL-2 receptor β and γ chains [48]. The highly affine heterotrimer binds IL-2, initiates IL-2 receptor β and γ chain-mediated signaling, maintains continuous T cell activation, and drives T cells into the division cycle for their proliferation and differentiation. Thus, CD25 marks the activation of T cells and CD44 is a receptor for the extracellular mechanism hyaluronan, a marker of activation and memory T cells, which is involved in T cell activation as a T cell activation co-stimulatory molecule that protects T cells from apoptosis and maintains T cell proliferation and lifespan [49]. It also binds to target cells, such as HA on the surface of tumor cells, and promotes the migration of lymphocytes to tumor cells. CD69 is a type II transmembrane glycoprotein belonging to the C-type lectin receptor family and is considered to be the earliest marker to emerge during T-cell activation, and not only that, but it is also involved in cell proliferation and differentiation, signal transduction and metabolic secretion [50,51]. In summary, CD25, CD44 and CD69 were used as markers of T-cell activation. The cellular experiments in which the drug intervention was administered in the presence of exogenous stimulation of $CD8^+$T cells with anti-CD3, CD28 antibodies and IL-2 for 24 h. To observe the effect of the drug on $CD8^+$T cell activation, flow cytometry assay analysis, which showed that the expression of CD25 and CD69 molecules on the surface of $CD8^+$T cells was significantly upregulated in AA mice, which is consistent with the pathogenesis of AA. This is consistent with the aberrant activation of $CD8^+$T cells in the pathogenesis of AA. However, CD44 expression was significantly downregulated in AA mice, consistent with the results of earlier clinical experiments [52]. CsA significantly downregulated the expression of CD25, CD44 and CD69, however, the effect of DNS on CD25 was not significant. The ISC group showed significant inhibition of the expression including all three activation markers. This indicates that DNS and CsA were able to inhibit $CD8^+$T cell activation. In addition to detecting surface activation molecules, mature CTL express a variety of surface molecules and secrete soluble factors, such as FasL and some cytokines INF-γ, TNF-α, perforin and granzyme that directly exert effector functions to modulates the efficiency of target cells killing and inducing apoptosis [6,7,33,34]. Moreover, TLR as the first line to defense plays the fascinating role in modulating the human immune responses at innate as well as adaptive levels directed the scientists to opt for these immune sensor proteins as suitable targets for developing chemotherapeutics and immunotherapeutics against cancer [11]. ELISA was used to quantify the functional cytokines, INF-γ, perforin and granzyme secreted by $CD8^+$T cells, and the results showed that the secretion of INF-γ, perforin and granzyme were significantly up-regulated by $CD8^+$T cells in AA mice, and DNS and CsA could inhibit cytokine secretion after drug administration intervention. Importantly, INF-γ, perforin and granzyme were significantly down-regulated in the ISC group significantly. In summary, the detection of surface immunophenotype and cytokine secretion of $CD8^+$T cells showed that DNS and CsA were able to inhibit the activation and function of $CD8^+$T cells.

In summary, our vitro experiment results showed that the ISC-treated effect was better than DNS-treated and CsA-treated effects, and the ISC initiated $CD8^+$T cell canonical and non-canonical autophagy through inhibiting mTORC1 activity to suppress the expression and activity of p300, which inhibits $CD8^+$T cell activation and effector cytokine secretion for treating AA. Autophagy is a two-edged sword; sometimes it can be helpful in some disease target cells mechanisms, but it can also occasionally be destructive. For instance, it promotes the resistance of cancer cells to chemotherapy, while excessive autophagy may lead to unintended cell death. However, our understanding of autophagy is growing quickly. It may soon be able to control autophagy to treat illness and improve health.

The strength of this experiment is that ISC can not only initiate autophagy in CD8+T cells through the classical postural pathway in vitro, but also constructed a cell model with high expression of mTORC1 on the basis of this experiment, which verified that ISC can also improve the autophagy defects and inhibit the function of CD8+T cells through the non-classical autophagy pathway and provided new ideas and theoretical support for the potential therapeutic targets of remittent disorders. However, this experiment lacked the support of clinical samples to verify the therapeutic effect of the drug on AA, and it was decided that make up for this deficiency in future studies on AA.

Ethics approval

This study was approved by the Animal Management and Ethics Committee of Tianjin Medical university (IRB2020-DW-189).

Funding

This study was supported by the National Natural Science Foundation of China (grant number 82004334 and 81973636).

Data availability

Data will be made available on request.

Disclosure statement

The authors report there are no competing interests to declare.

CRediT authorship contribution statement

Runfeng Ni: Writing – review & editing, Writing – original draft. **Liwei Fan:** Data curation, Conceptualization. **Haijin Wang:** Writing – review & editing, Writing – original draft. **Quan Zhang:** Investigation, Visualization. **Le Zhang:** Software, Validation. **Aidi Wang:** Supervision, Funding acquisition. **Baoshan Liu:** Supervision, Funding acquisition.

Declaration of competing interest

The authors declare the following financial interests/personal relationships which may be considered as potential competing interests: Baoshan Liu& Aidi Wang reports financial support was provided by National Natural Science Foundation of China. If there are other authors, they declare that they have no known competing financial interests or personal relationships that could have appeared to influence the work reported in this paper.

Acknowledgements

We thank the Basic Medical Research Center of Tianjin Medical University and Laboratory of Integrated Chinese and Western Medicine, Tianjin Medical University General Hospital (Tianjin, China) for their equipment support and technical guidance.

Appendix A. Supplementary data

Supplementary data to this article can be found online at https://doi.org/10.1016/j.heliyon.2024.e33755.

References

[1] E.F. Blommaart, et al., Phosphorylation of ribosomal protein S6 is inhibitory for autophagy in isolated rat hepatocytes, J. Biol. Chem. 270 (5) (1995) 2320–2326.
[2] C. Liu, et al., *TRAIL in CD8^{+}T cells from patients with severe aplastic anemia*, Int. J. Hematol. 106 (4) (2017) 490–499.
[3] I. Dikic, Z. Elazar, Mechanism and medical implications of mammalian autophagy, Nat. Rev. Mol. Cell Biol. 19 (6) (2018) 349–364.
[4] J. Huang, et al., Impaired autophagy in adult bone marrow CD34+Cells of patients with aplastic anemia: possible pathogenic significance, PLoS One 11 (3) (2016).
[5] Y. Xu, W. Wan, Acetylation in the regulation of autophagy, Autophagy 19 (2) (2023) 379–387.
[6] W. Qi, et al., Abnormal expression of histone acetylases in CD8+T cells of patients with severe aplastic anemia, J. Clin. Lab. Anal. 36 (4) (2022) e24339.
[7] W. Qi, et al., Abnormal histone acetylation of CD8(+) T cells in patients with severe aplastic anemia, Int. J. Hematol. 104 (5) (2016) 540–547.
[8] W. Wan, et al., mTORC1 phosphorylates acetyltransferase p300 to regulate autophagy and lipogenesis, Mol. Cell. 68 (2) (2017) 323–335 e6.
[9] X.L. Song, et al., Discorea nipponica saponins restore the Th17/Treg balance in aplastic anemia through the Notch/RBPJ kappa/FOXP3/ROR gamma t axis, J. King Saud Univ. Sci. 32 (2) (2020) 1664–1672.
[10] P. Behzadi, et al., The interleukin-1 (IL-1) superfamily cytokines and their single nucleotide polymorphisms (SNPs), J Immunol Res 2022 (2022) 2054431.
[11] S. Mukherjee, et al., Toll-like receptor-guided therapeutic intervention of human cancers: molecular and immunological perspectives, Front. Immunol. 14 (2023) 1244345.
[12] R. Ni, et al., A mouse model of irradiation and spleen-thymus lymphocyte infusion induced aplastic anemia, Hematology 27 (1) (2022) 932–945.
[13] K. Nishikawa, Y. Mezawa, T. Kobayashi, Bcat1 is controlled by Tsc2/mTORC1 pathway at expression levels and its deficiency together with Bcat2 inactivation suppresses the growth of a Tsc2(-/-) tumor cell line, Gene Cell. 28 (6) (2023) 447–456.
[14] P. Behzadi, R. Ranjbar, DNA microarray technology and bioinformatic web services, Acta Microbiol. Immunol. Hung. 66 (1) (2019) 19–30.
[15] M. Laplante, D.M. Sabatini, Regulation of mTORC1 and its impact on gene expression at a glance, J. Cell Sci. 126 (Pt 8) (2013) 1713–1719.
[16] S. Sciarretta, et al., New insights into the role of mTOR signaling in the cardiovascular system, Circ. Res. 122 (3) (2018) 489–505.
[17] I.H. Lee, T. Finkel, Regulation of autophagy by the p300 acetyltransferase, J. Biol. Chem. 284 (10) (2009) 6322–6328.
[18] J. Wu, et al., Molecular cloning and characterization of rat LC3A and LC3B–two novel markers of autophagosome, Biochem. Biophys. Res. Commun. 339 (1) (2006) 437–442.
[19] Y. You, et al., Contribution of autophagy-related gene 5 variants to acquired aplastic anemia in Han-Chinese population, J. Cell. Biochem. 120 (7) (2019) 11409–11417.
[20] G. Bjorkoy, et al., p62/SQSTM1 forms protein aggregates degraded by autophagy and has a protective effect on huntingtin-induced cell death, J. Cell Biol. 171 (4) (2005) 603–614.
[21] P. Codogno, M. Mehrpour, T. Proikas-Cezanne, Canonical and non-canonical autophagy: variations on a common theme of self-eating? Nat. Rev. Mol. Cell Biol. 13 (1) (2011) 7–12.
[22] K. Inoki, T. Zhu, K.L. Guan, TSC2 mediates cellular energy response to control cell growth and survival, Cell 115 (5) (2003) 577–590.
[23] H. Su, et al., VPS34 acetylation controls its lipid kinase activity and the initiation of canonical and non-canonical autophagy, Mol. Cell. 67 (6) (2017) 907–921 e7.
[24] Y. Kabeya, et al., LC3, a mammalian homologue of yeast Apg8p, is localized in autophagosome membranes after processing, EMBO J. 19 (21) (2000) 5720–5728.
[25] Z. Yang, D.J. Klionsky, Eaten alive: a history of macroautophagy, Nat. Cell Biol. 12 (9) (2010) 814–822.
[26] A.B. Novikoff, E. Essner, N. Quintana, Golgi apparatus and lysosomes, Fed. Proc. 23 (1964) 1010–1022.
[27] Y. Rikihisa, Glycogen autophagosomes in polymorphonuclear leukocytes induced by rickettsiae, Anat. Rec. 208 (3) (1984) 319–327.
[28] X. Qu, et al., Promotion of tumorigenesis by heterozygous disruption of the beclin 1 autophagy gene, J. Clin. Invest. 112 (12) (2003) 1809–1820.
[29] J.S. Carew, et al., Targeting autophagy augments the anticancer activity of the histone deacetylase inhibitor SAHA to overcome Bcr-Abl-mediated drug resistance, Blood 110 (1) (2007) 313–322.
[30] I.X. McLeod, W. Jia, Y.W. He, The contribution of autophagy to lymphocyte survival and homeostasis, Immunol. Rev. 249 (1) (2012) 195–204.
[31] J. Scopes, et al., Haemopoietic progenitor cells are reduced in aplastic anaemia, Br. J. Haematol. 86 (2) (1994) 427–430.
[32] S. Kordasti, et al., Functional characterization of CD4+T cells in aplastic anemia, Blood 119 (9) (2012) 2033–2043.
[33] L. Xing, et al., CD8+HLA-DR+T cells are increased in patients with severe aplastic anemia, Mol. Med. Rep. 10 (3) (2014) 1252–1258.
[34] M. Cicchini, V. Karantza, B. Xia, Molecular pathways: autophagy in cancer–a matter of timing and context, Clin. Cancer Res. 21 (3) (2015) 498–504.

[35] S.K. Vodnala, et al., T cell stemness and dysfunction in tumors are triggered by a common mechanism, Science 363 (6434) (2019).
[36] S.H. Ou-Yang, et al., Dioscorea nipponica Makino: a systematic review on its ethnobotany, phytochemical and pharmacological profiles, Chem. Cent. J. 12 (1) (2018) 57.
[37] L. Zhang, et al., Dioscin regulating bone marrow apoptosis in aplastic anemia, Drug Des. Dev. Ther. 16 (2022) 3041–3053.
[38] Y. Wang, et al., Effects of the total saponins from Dioscorea nipponica on immunoregulation in aplastic anemia mice, Am. J. Chin. Med. 43 (2) (2015) 289–303.
[39] T.H. Totterman, et al., Treatment of pure red-cell aplasia and aplastic anaemia with ciclosporin: long-term clinical effects, Eur. J. Haematol. 42 (2) (1989) 126–133.
[40] T. Hara, N. Mizushima, Role of ULK-FIP200 complex in mammalian autophagy: FIP200, a counterpart of yeast Atg 17? Autophagy 5 (1) (2009) 85–87.
[41] R. Huang, et al., Deacetylation of nuclear LC3 drives autophagy initiation under starvation, Mol. Cell. 57 (3) (2015) 456–466.
[42] T. Narita, B.T. Weinert, C. Choudhary, Functions and mechanisms of non-histone protein acetylation, Nat. Rev. Mol. Cell Biol. 20 (3) (2019) 156–174.
[43] X. Liu, et al., The structural basis of protein acetylation by the p300/CBP transcriptional coactivator, Nature 451 (7180) (2008) 846–850.
[44] L.M. Lasko, et al., Discovery of a selective catalytic p300/CBP inhibitor that targets lineage-specific tumours, Nature 550 (7674) (2017) 128–132.
[45] S. Sebti, et al., BAT3 modulates p300-dependent acetylation of p53 and autophagy-related protein 7 (ATG7) during autophagy, Proc. Natl. Acad. Sci. U. S. A. 111 (11) (2014) 4115–4120.
[46] W. Wu, et al., P300/HDAC1 regulates the acetylation/deacetylation and autophagic activities of LC3/Atg8-PE ubiquitin-like system, Cell Death Dis. 7 (1) (2021) 128.
[47] J.H. Shrimp, et al., Characterizing the covalent targets of a small molecule inhibitor of the lysine acetyltransferase P300, ACS Med. Chem. Lett. 7 (2) (2016) 151–155.
[48] M. Hashimoto, et al., PD-1 combination therapy with IL-2 modifies CD8(+) T cell exhaustion program, Nature 610 (7930) (2022) 173–181.
[49] B.F. Haynes, et al., CD44–a molecule involved in leukocyte adherence and T-cell activation, Immunol. Today 10 (12) (1989) 423–428.
[50] M. Shipkova, E. Wieland, Surface markers of lymphocyte activation and markers of cell proliferation, Clin. Chim. Acta 413 (17–18) (2012) 1338–1349.
[51] D. Cibrian, F. Sanchez-Madrid, CD69: from activation marker to metabolic gatekeeper, Eur. J. Immunol. 47 (6) (2017) 946–953.
[52] I. Bernard, G.J. Fournie, A. Saoudi, Genomics studies of immune-mediated diseases using the BN-LEW rat model, Methods Mol. Biol. 597 (2010) 389–402.